

Influence of spin correlations on band structure of magnetic semiconductors

J. Sinkkonen

Electron Physics Laboratory, Helsinki University of Technology, SF-02150 Espoo, Finland

(Received 24 March 1980; revised manuscript received 3 December 1980)

A perturbation treatment of the s - f interaction in ferromagnetic semiconductors is presented. The many-spin correlation functions are expressed in terms of connected correlation functions which are constructed by the mean-field theory. For the self-energy an integral equation is obtained which includes correlation effects. The method of calculation is closely connected with the coherent-potential approximation. As an application the density of states is shown in various cases by allowing the bandwidth to vary from broad- to narrow-band regime. The calculation is limited to the paramagnetic phase. Correlation effects are seen as temperature-dependent changes in the density of states.

I. INTRODUCTION

In magnetic semiconductors conduction electrons are different from the electrons responsible for magnetism. Magnetic moments arise from localized electrons which partially fill the ionic d or f shells. The moments are situated in a regular lattice and are coupled to each other by the superexchange or indirect-exchange mechanisms. The conduction electrons are ordinary band electrons. The conduction band is separated by an energy gap from the energy of the magnetic electrons.

The interesting physical properties of magnetic semiconductors are a consequence of the exchange interaction between the conduction electrons and the moments of the magnetic lattice. In ferromagnetic semiconductors this interaction is responsible for the large red shift of the absorption edge near and below the Curie temperature T_C , the giant resistivity peak near T_C , and the extraordinary large negative magnetoresistance.¹⁻⁴

The theory of magnetic semiconductors is influenced by three important ingredients: the magnitude of the conduction-band width W , the magnitude of the exchange interaction J between the conduction electrons and the magnetic moments, and the state of ordering of the magnetic lattice. W may vary from zero to a few electron volts. J is typically a fraction of electron volt. The magnetic excitation energies are always small compared to the electronic energies. Thus W and J define the large part of the system. However, the state of ordering of the magnetic lattice has a large influence on electronic energies via the exchange interaction.

Exact solution for an ideal paramagnetic semiconductor is only known in the zero-bandwidth case. When $W = 0$, the Hamiltonian is diagonal in the localized basis, and the problem reduces to the case of an ion with an extra electron. As a result, the band energy is split by the exchange interaction into two multiplets. These present the situa-

tion where the conduction-electron spin is oriented in the same or opposite direction compared with the ionic magnetic moment. The band splitting is independent of the state of magnetic lattice, and consequently the structure of conduction band is independent of temperature.

The zero-bandwidth limit gives a natural starting point for the theory of narrow-band magnetic semiconductors⁵ characterized by the condition $W \ll J$. Owing to the nonvanishing W , the conduction electron is no longer localized on a particular site, and the state of magnetic lattice influences the electronic spectrum. The method of calculation in Ref. 5 is based on a canonical transformation. It can be generalized to any order in W/J , but unfortunately it leads to a complicated system which has been solved only in the limit $W \ll J$. In the narrow-band regime, the bands originating from the two multiplets remain separate in energy at all temperatures.

Another possibility is to start from the broad-band regime, $W \gg J$. In this case the exchange interaction between conduction electrons and magnetic moments is treated as a perturbation. In first order the conduction band is split in ferromagnetic region into two spin-polarized subbands owing to the long-range order of the magnetic system. The second-order corrections depend on a two-spin correlation function, i.e., they reflect the role of short-range order. These corrections are large near and above T_C and must be included in order to adequately explain the shift of the absorption edge.⁶⁻¹⁰ Continuing the theory to higher orders introduces higher-order spin-correlation functions which are poorly understood. The two-spin correlation function is fairly well known both from experiment and theory; some theoretical studies exist for three- and four-spin correlation functions, but the higher-order functions are almost unknown. This is why the existing theories are mostly different types of second-order versions,⁶⁻¹⁰ which can be satisfactory only

in $W \gg J$ limit.

For arbitrary values of W and J there exist two kinds of treatments. In the first one the method of moments is utilized.¹¹⁻¹³ Here one assumes a structure for conduction band and the fitting parameters are adjusted by calculating the relevant number of moments. The actual applications of the method are based on the detailed solution of the zero-bandwidth case. Thus their validity for more general cases may be questioned. Furthermore, the accuracy of this method always depends on the validity of the initial assumption for the band structure, a matter which is very difficult to check. The second type of treatments uses the coherent potential approximation (CPA).¹⁴⁻¹⁶ This method was originally developed for random binary alloys.¹⁷⁻²⁰ In the present case, the random atomic energy "seen" by an electron at a particular lattice site is one of the two multiplet energies discussed above. Thus the CPA formalism is directly applicable. It is known that the CPA is fairly good for any values of bandwidth and scattering potential. In the present case the validity is, however, limited to high temperatures, since the magnetic moments are randomly oriented only in the high-temperature region. When the temperature decreases the magnetic moments become correlated. The importance of the correlation effects on band structure is already seen in the weak-coupling theories.⁶⁻¹⁰

The aim of this paper is to develop a CPA-type theory which includes correlations between the magnetic moments. The theory is presented in Sec. II using ordinary diagrammatic methods. The correlation functions between the magnetic moments are expressed in terms of so-called connected correlation functions which are derivatives of local magnetization with respect to the exciting magnetic field. In Sec. III the method is applied to various magnetic semiconductors by allowing the bandwidth to vary from broad to narrow-band regimes.

II. PERTURBATION THEORY

According to the s - f model the Hamiltonian which describes conduction electrons interacting with the moments of the magnetic lattice is given by

$$H = \sum_{\nu} E_{\nu} a_{\nu}^{\dagger} a_{\nu} - \frac{1}{N} \sum_{\nu, \nu', i} \mathfrak{J}(\nu, \nu', i) \cdot \vec{S}_i a_{\nu}^{\dagger} a_{\nu'} + H_M. \quad (1)$$

The first term is the single-band Hamiltonian for conduction electrons, the second one the exchange interaction between conduction electrons and the localized magnetic moments, and the last one the pure magnetic Hamiltonian. The index ν denotes both the wave vector \vec{k} and the spin index σ of a band electron. In the exchange part N is the number of unit cells and \mathfrak{J} is of the form

$$\mathfrak{J}(\nu, \nu', i) = J e^{i(\vec{k}' - \vec{k}) \cdot \vec{R}_i} 2 \langle \sigma | \vec{s} | \sigma' \rangle. \quad (2)$$

Here J is the exchange integral, \vec{R}_i the lattice site vector associated with the localized spin \vec{S}_i , and \vec{s} the conduction-electron spin. H_M is the ordinary Heisenberg Hamiltonian

$$H_M = - \sum_{i, j} I(\vec{R}_i - \vec{R}_j) \vec{S}_i \cdot \vec{S}_j + g \mu_B \sum_i \vec{S}_i \cdot \vec{B}_i, \quad (3)$$

where I is the exchange parameter and \vec{B}_i the flux density of a magnetic field at the point \vec{R}_i .

It is straightforward to write down an expansion for the Zubarev Green's function^{21, 22} $G_{\mu} = \langle\langle a_{\mu}; a_{\mu}^{\dagger} \rangle\rangle$ in powers of J . The expansion is slightly simplified when one first subtracts from the exchange interaction the part arising from the thermal average of lattice spins. This means that one starts with the spin-polarized band picture. An additional simplification comes from the fact that the magnetic excitation energies are small compared to the electron energies. Consequently, the magnetic lattice can be regarded as a static system in the electronic time scale. Thus H_M and the commutators of lattice spins can be neglected in the equation of motion for G . This results in an expansion

$$G_{\mu} = G_{\mu}^{(0)} \left\{ \delta_{\mu, \mu'} - \frac{1}{N} \sum_{\nu, i} G_{\nu}^{(0)} \mathfrak{J}(\mu, \nu, i) \cdot \left[\langle \vec{\xi}_i \rangle \delta_{\nu, \mu'} - \frac{1}{N} \sum_{\nu', j} G_{\nu'}^{(0)} \mathfrak{J}(\nu, \nu', j) \cdot \left(\langle \vec{\xi}_j \vec{\xi}_i \rangle \delta_{\nu', \mu'} - \frac{1}{N} \sum_{\nu'', m} G_{\nu''}^{(0)} \mathfrak{J}(\nu', \nu'', m) \cdot \{ \langle \vec{\xi}_m \vec{\xi}_j \vec{\xi}_i \rangle \delta_{\nu'', \mu'} - \dots \} \right) \right] \right\}. \quad (4)$$

Here $G^{(0)}$ is the electron propagator associated with the spin-polarized bands. The single bracket $\langle \dots \rangle$ denotes the thermal average and the reduced spin $\vec{\xi}_i$ is defined by

$$\vec{\xi}_i = \vec{S}_i - \langle \vec{S}_i \rangle. \quad (5)$$

In order to develop a perturbation theory in all orders in J , it is necessary to find a representation for the higher-order spin correlation functions occurring in Eq. (4). In general, the fluctuations can be expressed in terms of derivatives with respect to acting force. This introduces the

connected correlation functions.^{20,23} For a magnetic system they are defined⁹ as derivatives of local magnetization $\langle S_i^\alpha \rangle$ with respect to exciting magnetic field B_j^β :

$$C^{(n+1)}(S_1^\alpha, S_2^\beta, \dots, S_{n+1}^\gamma) = \left(-\frac{k_B T}{g \mu_B} \right)^n \frac{\partial^n \langle S_1^\alpha \rangle}{\partial B_{n+1}^\gamma \dots \partial B_2^\beta}, \quad (6)$$

where the thermal average of S_1^α is given by

$$\begin{aligned} \langle \vec{\xi}_1 \vec{\xi}_2 \vec{\xi}_3 \dots \vec{\xi}_n \rangle &= C^{(n)}(\vec{S}_1, \dots, \vec{S}_n) + \sum_p' [C^{(p)}(\vec{S}_1, \dots, \vec{S}_p) C^{(n-p)}(\vec{S}_{p+1}, \dots, \vec{S}_n) + \text{perm.}] \\ &+ \sum_{p_1, p_2}' [C^{(p_1)}(\vec{S}_1, \dots, \vec{S}_{p_1}) C^{(p_2)}(\vec{S}_{p_1+1}, \dots, \vec{S}_{p_1+p_2}) C^{(n-p_1-p_2)}(\vec{S}_{p_1+p_2+1}, \dots, \vec{S}_n) + \text{perm.}] + \dots, \quad (8) \end{aligned}$$

where perm. represents terms resulting from permutations of the spins. In other words, the right-hand side is generated by all different partitions of n spins. There are $n!/[p!(n-p)!]$ terms of the type $C^{(p)}C^{(n-p)}$, $n!/[p_1!p_2!(n-p_1-p_2)!]$ terms of the type $C^{(p_1)}C^{(p_2)}C^{(n-p_1-p_2)}$, etc. The prime on the summation denotes that the $C^{(1)}$ terms are to be excluded, since they are already present in the product of $\vec{\xi}_i$'s in the left-hand side of Eq. (8).

It is convenient to use the Fourier-transformed C functions

$$\begin{aligned} C^{(n)}(\vec{S}(\vec{q}_1), \dots, \vec{S}(\vec{q}_n)) \\ = \sum_{\vec{R}_1, \dots, \vec{R}_n} e^{i\vec{q}_1 \cdot \vec{R}_1} \times \dots \times e^{i\vec{q}_n \cdot \vec{R}_n} \\ \times C^{(n)}(\vec{S}_1, \dots, \vec{S}_n). \quad (9) \end{aligned}$$

Since the correlation functions depend only on mutual distances between the spins, the Fourier transforms conserve the wave vectors, i.e.,

$$\begin{aligned} C^{(n)}(\vec{S}(\vec{q}_1), \dots, \vec{S}(\vec{q}_n)) \\ = \delta_{\vec{q}_1 + \dots + \vec{q}_n, 0} C^{(n)}(\vec{S}(\vec{q}_1), \dots, \vec{S}(\vec{q}_n)). \quad (10) \end{aligned}$$

Using Eqs. (8) and (9) the expansion for G is conveniently described by diagrams. The corresponding expansion for the self-energy is shown in Fig. 1 up to sixth order in J . The double horizontal line denotes the Green's function G and the dashed line the s - f interaction. With the interaction line there is associated a factor $-\vec{J}(\vec{k}\sigma, \vec{k}'\sigma') = -J2\langle \sigma | \vec{s} | \sigma' \rangle$, with the cross a factor $C^{(p)}(\dots, \vec{S}(\vec{k} - \vec{k}', \dots))$ and a proper scalar product of \vec{J} and $C^{(p)}(\dots, \vec{S}(\vec{k} - \vec{k}', \dots))$ is implied. The diagrams are ordered into columns according to the number of C factors. The diagrams in the first column represent scattering from independent spin clus-

$$\langle S_1^\alpha \rangle = \text{Tr}(e^{-H_M/k_B T} S_1^\alpha) / \text{Tr}(e^{-H_M/k_B T}). \quad (7)$$

When the derivatives in Eq. (6) are calculated, it is consistent to regard the magnetic system as a classical one, since the commutators of lattice spins have already been neglected in the expansion of G . With the help of Eqs. (6) and (7) the n th-order spin correlation function can be expressed in terms of C functions as follows:

ters. The crossed diagrams, for instance diagrams of the type $C^{(p)}C^{(n-p)}$, represent such a scattering from two lower-order clusters which does not reduce into a repeated scattering from these clusters.

The next task is to construct the C functions explicitly. The simplest way is to calculate the derivatives in Eq. (6) by the mean-field theory. This method was used by de Gennes and Villain²⁴ to derive the wave-vector-dependent susceptibility, i.e., $C^{(2)}$. Here we simply generalize the method to higher orders. The calculation is performed in the Appendix by considering only correlations between the z components. From Eqs. (A4), (A9), and (A11)

$$\begin{aligned} C^{(1)}(S^z(\vec{q}_1)) &= -NSB_S(x)\delta_{\vec{q}_1, 0}, \\ C^{(2)}(S^z(\vec{q}_1), S^z(\vec{q}_2)) &= NS^2 \frac{\partial B_S}{\partial x} f(\vec{q}_1)\delta_{\vec{q}_1 + \vec{q}_2, 0}, \quad (11) \end{aligned}$$

$$\begin{aligned} C^{(n)}(S^z(\vec{q}_1), \dots, S^z(\vec{q}_n)) \\ = N(-S)^n \frac{\partial^{n-1} B_S}{\partial x^{n-1}} f(\vec{q}_1) \times \dots \times f(\vec{q}_n) \\ \times \delta_{\vec{q}_1 + \dots + \vec{q}_n, 0}, \quad n > 2. \end{aligned}$$

The correlation effects are included in $f(\vec{q})$ which is given by

$$f(\vec{q}) = 1 / \left(1 - \frac{2S^2}{k_B T} I(\vec{q}) \frac{\partial B_S}{\partial x} \right). \quad (12)$$

In Eq. (11) $C^{(1)}$ is just the magnetization in the mean-field theory. It is known to be rather good at all temperatures. $C^{(2)}$ is the wave-vector-dependent longitudinal susceptibility. In paramagnetic phase it takes the well-known Ornstein-Zernike form in the long-wavelength limit. This is known to be realistic above T_c . At T_c , $C^{(2)}$ is

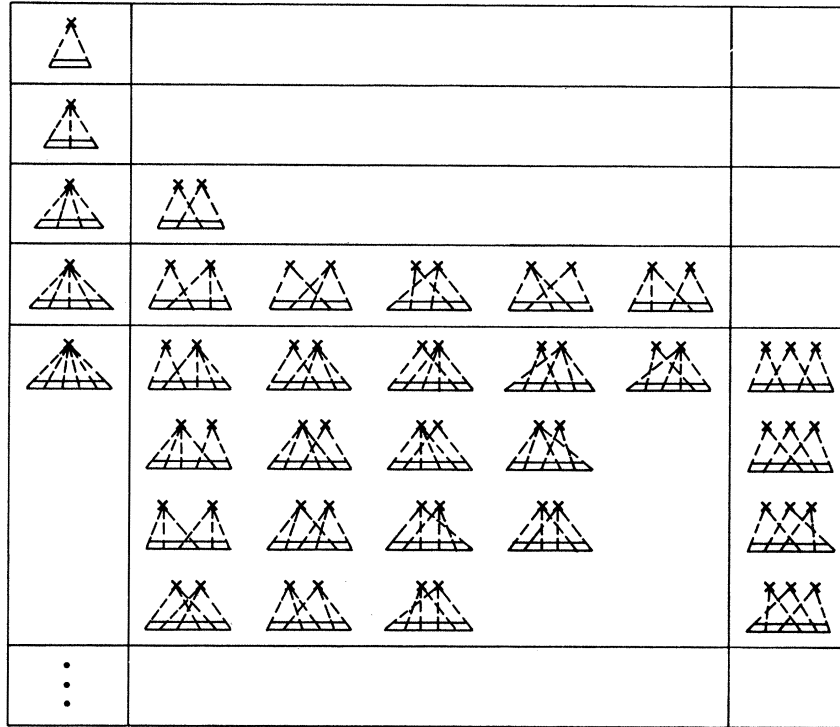


FIG. 1. Expansion of self-energy up to sixth order in J .

divergent as it should be. However, the critical exponent differs slightly from the correct value. Furthermore it is known that far below T_C , $C^{(2)}$ decreases too rapidly. The higher-order functions are just generalizations of these two. Their validity depends on the accuracy of the mean-field theory for the local magnetization. Essentially in this theory the spins are assumed to be dynamically independent, which can be expected to be realistic at least in the paramagnetic phase.

In the high-temperature limit $f(\vec{q}) \rightarrow 1$, i.e., the effect of correlation vanishes, and Eq. (11) reduces to the exact result for an ideal paramagnet. Thus we see that the high-temperature limit of the C functions is correct.

By considering the same spin moments, Eq. (11) leads to the sum rules

$$\frac{1}{N} \sum_{\vec{q}} f(\vec{q}) = 1,$$

$$\frac{1}{N^n} \sum_{\vec{q}_1, \dots, \vec{q}_n} f(\vec{q}_1) \times \dots \times f(\vec{q}_n) f(\vec{q}_1 + \dots + \vec{q}_n) = 1$$

$n \geq 2.$ (13)

It is obvious that these sum rules are exactly satisfied only in the high-temperature limit. However, deriving $I(\vec{q})$ from nearest-neighbor exchange parameters, it turns out that the first sum

rule is satisfied within an accuracy of 10% in the whole paramagnetic temperature region. Replacing $f(\vec{q})$ by its long-wavelength form, the error of the first sum rule is always less than 25%. A similar conclusion applies to the higher-order sum rules. Thus it is seen that the sum rules are never badly violated.

Consider now the summation of diagrams in Fig. 1. Let us first treat the Ising part of the s - f interaction, since it involves only correlations between the z components. A complication arises from the fact that $C^{(2)}$ in Eq. (11) is structurally different from the higher-order C functions. It is instructive to first replace $C^{(2)}$ by a more symmetric form

$$C^{(2)} \rightarrow NS^2 \frac{\partial B_z}{\partial x} f(\vec{q}_1) f(\vec{q}_2) \delta_{\vec{q}_1 + \vec{q}_2, 0},$$

and correct the result afterwards. The diagrams in the first column are easily summed. They lead to an integral equation for the self-energy. Additionally we select from crossed diagrams those parts which are structurally equivalent to the diagrams in the first column. Consider as an example a particular diagram of the type $C^{(p)} C^{(n-p)}$. Owing to the C functions there are two wave-vector-conserving δ functions. The diagram is of the form

$$\begin{aligned} & \sum_{\vec{q}_1, \dots, \vec{q}_n} \dots \delta_{\vec{q}_1 + \dots + \vec{q}_p, 0} \delta_{\vec{q}_{p+1} + \dots + \vec{q}_n, 0} \\ &= \frac{1}{N} \sum_{\vec{R}} \sum_{\vec{q}_1, \dots, \vec{q}_n} \dots e^{i(\vec{q}_1 + \dots + \vec{q}_p) \cdot \vec{R}} \delta_{\vec{q}_1 + \dots + \vec{q}_n, 0}. \end{aligned} \quad (14)$$

In the \vec{R} summation the term $\vec{R} = 0$ is just the part which is of the same type as the n th-order diagram in the first column. Thus we pick out the $\vec{R} = 0$ term from Eq. (14). Using repeatedly Eq. (14) we are able to select the desired parts from more complicated crossed diagrams. This method of treating the crossed diagrams is characteristic to the CPA.²⁰ In wave-vector space the δ functions are replaced by a less restrictive condition as seen from Eq. (14). This is allowed provided that the quantities to be summed are slowly varying in wave vector. Taking the Fourier transform into \vec{R} space, the essential condition for the validity of the method is that $G(\vec{R})$ be rapidly decreasing beyond $\vec{R} \neq 0$. This condition implies that there are no undamped poles of the Green's function close to band edges. This is the basic limitation of the CPA. As a consequence the CPA always yields a relatively smooth spectrum.

To calculate the contribution from a given row, we have to sum the combination of coefficients of the C functions. Unfortunately there exists no general expression for the number of crossed diagrams of given type. This difficulty can be overcome by using the method of Leath.²⁵ In this method the contribution of all reducible diagrams is added to the sum of a given row, and is subtracted afterwards. However, the reducible diagrams are in each step treated as crossed diagrams. Denote by $T^{(n)}$ the sum of all n th-order diagrams including also the reducible diagrams. In the present approximation the \vec{q} dependence of $T^{(n)}$ is given by the n th-order diagram in the first column of Fig. 1, and we have to determine the coefficient associated with $T^{(n)}$. This coefficient can be calculated for the Ising part, but it is even simpler to find it for the full s - f interaction in the paramagnetic phase: When $\langle \vec{S}_i \rangle = 0$, the Green's function is independent of spin. The perturbation is proportional to $2\vec{s} \cdot \vec{S}_i$. The internal summation over the electron-spin indices can be performed by using the identity of Dirac:

$$2(\vec{s} \cdot \vec{S}_i)2(\vec{s} \cdot \vec{S}_j) = \vec{S}_i \cdot \vec{S}_j + 2i\vec{s} \cdot (\vec{S}_i \times \vec{S}_j). \quad (15)$$

The last term in Eq. (15) can be dropped. It arises from the commutator of electron-spin operators and is in fact cancelled by the same term in the expansion of G . Because the spin system is completely isotropic in the paramagnetic phase, the correlation functions between any spin components must have the same \vec{q} dependence as the

correlation functions between the z components. In other words, Eq. (11) applies to all C functions, except that the derivatives of Brillouin function are to be replaced by some other coefficients. Furthermore, all these coefficients are constant in the paramagnetic phase. Thus, we can take the high-temperature limit, where only the same spin moment occurs in the expansion of $T^{(n)}$. With the help of Eqs. (8) and (15) it is seen that the coefficient associated with $T^{(n)}$ is $[S(S+1)]^{n/2}$ if n is even and 0 otherwise.

By summing up all rows an integral equation for T is obtained:

$$\begin{aligned} T_{\vec{k}, \vec{k}} = & \frac{1}{N} \sum_{\vec{q}} K(\vec{k}' - \vec{q}) G_{\vec{q}} K(\vec{q} - \vec{k}) \\ & + \frac{1}{N^2} \sum_{\vec{q}, \vec{q}'} K(\vec{k}' - \vec{q}) G_{\vec{q}} K(\vec{q} - \vec{q}') G_{\vec{q}'} T_{\vec{q}', \vec{k}}. \end{aligned} \quad (16)$$

T is given by the diagonal element $T_{\vec{k}, \vec{k}}$. In Eq. (16)

$$K(\vec{q}) = JSf(\vec{q}), \quad (17)$$

where $[S(S+1)]^{1/2}$ is replaced by S . This is consistent, because through the calculation the magnetic system is treated essentially as a classical spin system. This is equivalent to the case $S > 1$.

The reducible diagrams to be subtracted from T are shown in Fig. 2. The crosses are connected with dotted lines to indicate that these diagrams are to be treated in the same way as the crossed diagrams were done in the calculation of T . Regarding the self-energy Σ as a function of its internal propagator each column can be summed separately as shown by Leath.²⁵ With the help of Fig. 2 one obtains

$$\begin{aligned} T(G) &= \Sigma(G') / \left(1 - \frac{1}{N} G \Sigma(G')\right), \\ G' &= G / \left(1 - \frac{1}{N} \Sigma(G')G\right). \end{aligned} \quad (18)$$

Equation (18) is to be understood as a matrix equation, i.e., G is a diagonal matrix with components $G_{\vec{q}}$, and T and Σ are square matrices with components $T_{\vec{q}, \vec{q}}, \Sigma_{\vec{q}, \vec{q}}$, etc. Now change $G \rightarrow X$ such that $G' \rightarrow G$. Equation (18) gives then $\Sigma = \Sigma(G)$ in terms of $T(X)$. From Eq. (16) we finally obtain an equation for the self-energy,

$$\Sigma + \frac{1}{N} \Sigma G \Sigma = \frac{1}{N} K G K, \quad (19)$$

or in component form

$$\Sigma_{\vec{q}, \vec{k}} + \frac{1}{N} \sum_{\vec{q}'} \Sigma_{\vec{k}', \vec{q}'} G_{\vec{q}'} \Sigma_{\vec{q}, \vec{k}} = \frac{1}{N} \sum_{\vec{q}} K(\vec{k}' - \vec{q}) G_{\vec{q}} K(\vec{q} - \vec{k}). \quad (20)$$

Next we have to consider corrections to the self-

⋮			
T	$\Sigma(G) - \Sigma(G')$	$-\Sigma(G')G \Sigma(G')$	$-\Sigma(G')G \Sigma(G')G \Sigma(G') \dots$

FIG. 2. Calculation of self-energy: Diagrams included in T are shown in the first column and the reducible diagrams to be subtracted from T in higher columns.

energy arising from the true $C^{(2)}$. It is essential for the present method of calculation that the \vec{q} dependence of diagrams must show simple structure in order for us to be able to convert the sum of diagrams into an integral equation. The crossed diagrams involving true $C^{(2)}$ break this simple structure considered. Thus we are forced to additional approximations. A very useful approximation is achieved by calculating the Σ matrix from Eq. (19) and by deriving then the self-energy from the equation

$$\Sigma_{\vec{k}} = \frac{1}{N} \sum_{\vec{q}} \Sigma_{\vec{k}, \vec{q}} \tag{21}$$

The expansion of self-energy starts now from the correct second-order term. Furthermore, this approximates better the crossed diagrams containing $C^{(2)}$. Equation (21) implies that in the higher-order C functions one of the $f(\vec{q})$'s is replaced by 1, i.e., by its average over \vec{q} . This results in an important advantage that all the sum rules are automatically satisfied once $f(\vec{q})$ is scaled to satisfy $(1/N) \sum_{\vec{q}} f(\vec{q}) = 1$. The sum rules reflect the fact that the magnitude of each lattice spin is fixed. In order to avoid unphysical solutions, it is important that the sum rules are exactly satisfied. As a consequence of the proper

account of sum rules the present method yields the correct result in the zero-bandwidth case, within the approximation $S > 1$.

At high temperatures the right-hand side of Eq. (20) is independent of wave vector. Consequently $\Sigma_{\vec{k}, \vec{k}}$ is also independent of \vec{k} and \vec{k}' , and the self-energy is given by

$$\Sigma = J^2 S^2 G(0) / [1 + \Sigma G(0)], \tag{22}$$

where

$$G(0) = \frac{1}{N} \sum_{\vec{q}} G_{\vec{q}} \tag{23}$$

This is just the ordinary CPA result of Rangette *et al.*¹⁴ for large S . Equations (19)–(21) are the main result of this paper. They determine a CPA-type self-energy which includes the effect of correlation between the scatterers. There are some formal similarities between the present treatment and the existing CPA theories for liquid and amorphous materials.^{26–28} These theories involve the atomic correlation functions. In Refs. 26–28 these functions are constructed by Kirkwood's superposition principle as symmetric products of two-atom correlation functions. The spin-correlation functions in Eq. (11) are different from Kirkwood's correlation functions, and consequently

the final equation for self-energy differs also from those given in Refs. 26–28.

III. RESULTS AND DISCUSSION

Using Eqs. (20)–(21) and taking into account the sum rule for $f(\vec{q})$ one obtains for the self-energy $\Sigma_{\vec{k}}$ an equation

$$\Sigma_{\vec{k}} + \frac{1}{N} \sum_{\vec{q}} \Sigma_{\vec{k}-\vec{q}} G_{\vec{q}} \Sigma_{\vec{q}} = \frac{1}{N} JS \sum_{\vec{q}} K(\vec{k}-\vec{q}) G_{\vec{q}}. \quad (24)$$

The right-hand side of Eq. (24) is just the second-order self-consistent self-energy considered previously in Ref. 9. In semiconductors the states close to the bottom of the band are the most important ones. For these states it is then sufficient to study the solution in the long-wavelength region, where the self-energy is, in the first approximation, independent of wave vector. Then Eq. (24) reduces into an algebraic equation

$$\Sigma + \Sigma^2 G(0) = JS \frac{1}{N} \sum_{\vec{q}} K(\vec{q}) G_{\vec{q}}, \quad (25)$$

which is easier to solve. Let us specifically consider the solution of Eq. (25) for europium chalcogenides such as EuS and EuO, which are the best studied among the ferromagnetic semiconductors. In the paramagnetic phase the long-wavelength expression for $f(\vec{q})$ reads

$$f(\vec{q}) = \lambda \frac{12T}{T_C} \frac{1}{\kappa^2 + a^2 q^2}, \quad (26)$$

where λ is the scaling parameter to be chosen such that $(1/N) \sum_{\vec{q}} f(\vec{q}) = 1$, $\kappa^2 = 12(T/T_C - 1)$, and a is the lattice constant. In other words $f(\vec{q})$ is of the Ornstein-Zernike form. In \vec{R} space it describes exponentially decreasing correlation between the spins, the quantity a/κ being the correlation length. The original conduction band is simply taken to be a truncated free-electron band characterized by the effective mass m^* . This is consistent in the long-wavelength limit. As the result of these approximations the accuracy of the solution is best in the low-energy region, but in particular the high-energy edge of the band is only qualitatively described.

Figure 3 shows the calculated density of states. The exchange energy JS is chosen to be 0.33 eV, which is a typical value for europium chalcogenides. The effective mass is varied to cover the broad ($m^* = m_0$), intermediate ($m^* = 3m_0$), and narrow ($m^* = 10m_0$) band regimes. The effect of correlation is seen as the temperature dependence of density of states. In the broad-band case, in Fig. 3(a), the band edges undergo temperature-dependent shifts. The upper edge shows a red shift, i.e., it shifts to lower energies with decreasing temperature, while the lower edge shows a blue

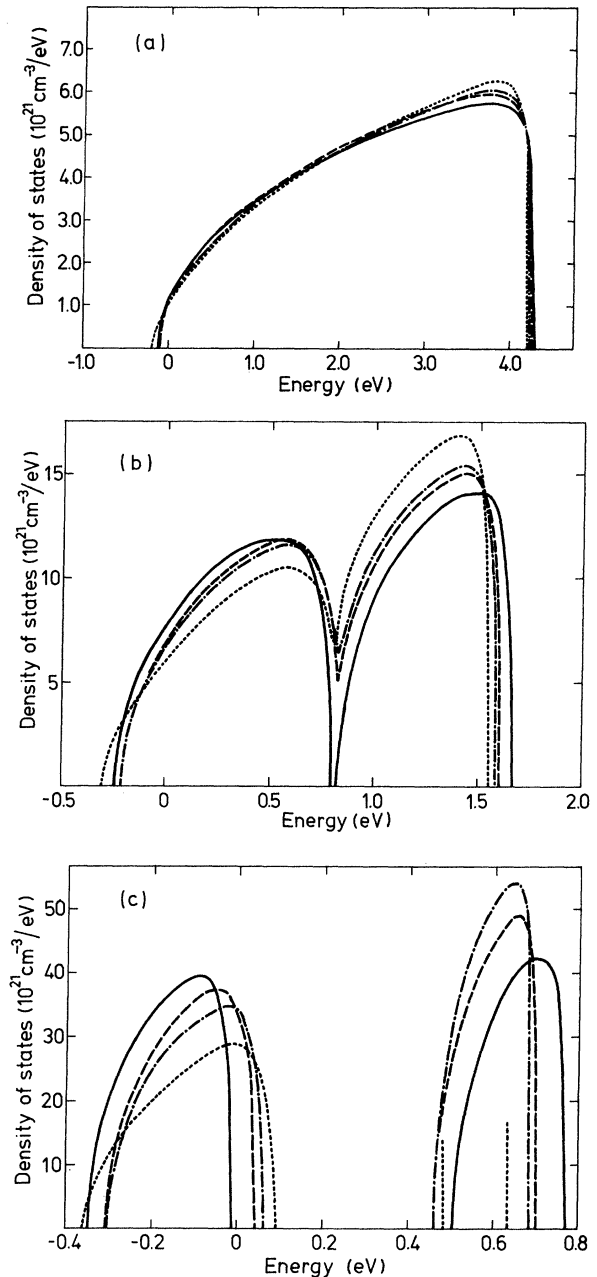


FIG. 3. Density of states per spin in the paramagnetic phase for (a) $m^* = m_0$, (b) $m^* = 3m_0$, and (c) $m^* = 10m_0$. The solid line corresponds to the temperature $T = 20T_C$, the dashed line to $T = 5T_C$, the dot-dashed line to $T = 3T_C$, and the dotted line to $T = 1.1T_C$.

shift at higher temperatures followed by a red shift below $3T_C$. As a result the total bandwidth decreases first with decreasing temperature and then below $3T_C$ increases again. In the intermediate case, in Fig. 3(b), the band is split into two subbands at high temperatures. The striking effect of correlations is that the band gap closes

again when temperature decreases. In the narrow-band case, in Fig. 3(c), the two subbands remain always separate in energy. The bandwidth of the lower subband increases with decreasing temperature, whereas the upper band shows the opposite behavior. For the upper subband the imaginary part of the self-energy is small compared to the real part. This introduces numerical instabilities in the solution particularly near T_C . This is why in Fig. 3(c) only the position of the upper subband is indicated at $T = 1.1T_C$.

If the bandwidth still decreases the density of states becomes less temperature dependent. In the extremal zero-bandwidth case Eq. (25) predicts two peaks for the density of states centered in energy at $\pm JS$, which is the exact result.

Figure 4 shows the low-energy band edge as a function of temperature. The blue shift in the region $T > 5T_C$ is of the order of 10^{-4} eV/K in all cases. The red shift in the region $T_C \leq T < 3T_C$ decreases with decreasing bandwidth.

The results of the broad-band case are close to those predicted by the second-order self-consistent theory.⁹ In particular, the temperature dependence of the low-energy band edge compares well with the observed shift of the absorption edge in europium chalcogenides. However, the interpretation of the optical absorption spectrum by means of the calculated density of states meets with difficulties. It is generally accepted that in europium chalcogenides the first optical transition is from the localized $4f$ level to the $5d$ -type conduction band. The absorption coefficient depends on the momentum matrix element and on the joint density of states. It is customary to regard the momentum matrix element as energy independent. Since the initial state is well localized, the absorption coefficient should be directly proportional to the conduction-band density of states. According to the energy-band calculations^{29,30} the d bands are broad having the width about 5 eV. Thus the absorption coefficient should have a structure

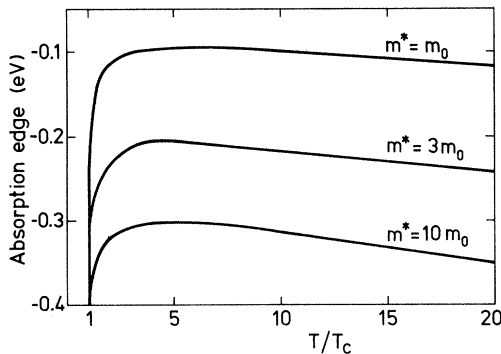


FIG. 4. Absorption edge as a function of temperature.

shown in Fig. 3(a). However, in all europium chalcogenides the absorption coefficient shows first a peak of width 1 eV. There are attempts to explain this peak in terms of excitonic transition.³ In heavily doped materials the exciton should disappear owing to the increased screening, but in experiments no effect of doping is seen. Thus the peak seems to indicate a relatively narrow conduction band of width 1 eV.^{31,32} However, according to the present theory a band of this width should be split into two separate subbands as shown in Fig. 3. No splitting is seen in the absorption coefficient and the situation remains controversial.

Obviously a more careful interpretation of the absorption coefficient is needed. The momentum matrix element is energy independent only in the framework of the lowest-order effective-mass theory. It implies that both the initial and the final states belong to broad bands. In the present case the initial state is well localized for which the lowest-order effective-mass theory does not apply. A well-known example of the case where the momentum matrix element is energy dependent is the transition from a localized impurity state to band. This can be handled by the ordinary effective-mass theory, which predicts that the momentum matrix element decreases at higher energies and the resulting absorption coefficient shows a peaked structure.³³ Thus in europium chalcogenides the conduction band may be broad in accordance with the band calculations, and the peak in absorption coefficient may be caused by the energy dependence of the momentum matrix element.

ACKNOWLEDGMENT

I wish to express my gratitude to Professor T. Stubb for his interest and help at different stages of this work and to the Academy of Finland and the Swedish Academy of Engineering Sciences in Finland for financial support.

APPENDIX: CALCULATION OF THE C FUNCTIONS

The magnetic Hamiltonian reads

$$H_M = - \sum_{i,j} I(\vec{R}_i - \vec{R}_j) \vec{S}_i \cdot \vec{S}_j + g\mu_B \sum_i \vec{S}_i \cdot \vec{B}_i. \quad (A1)$$

By definition, the thermal average of a component of the spin operator is

$$\langle S_i^\alpha \rangle = \text{Tr}(e^{-H_M/k_B T} S_i^\alpha) / \text{Tr}(e^{-H_M/k_B T}). \quad (A2)$$

The connected correlation functions⁹ are obtained as derivatives of $\langle S_i^\alpha \rangle$ with respect to the field B_j^β :

$$C^{(n+1)}(S_1^\alpha, S_2^\beta, \dots, S_{n+1}^\gamma) = \left(-\frac{k_B T}{g\mu_B} \right)^n \frac{\partial^n \langle S_1^\alpha \rangle}{\partial B_{n+1}^\gamma \dots \partial B_2^\beta}. \quad (A3)$$

According to the mean-field theory

$$\begin{aligned} \langle \vec{S}_i \rangle &= -SB_S(x_i) \vec{u}_i, \\ x_i &= \frac{g\mu_B S}{k_B T} |\vec{B}_{\text{eff}}(\vec{R}_i)|, \\ \vec{B}_{\text{eff}}(\vec{R}_i) &= -\frac{2}{g\mu_B} \sum_j I(\vec{R}_i - \vec{R}_j) \langle \vec{S}_j \rangle + \vec{B}_i. \end{aligned} \quad (\text{A4})$$

Here B_S denotes the Brillouin function, \vec{u}_i the unit vector in the direction of $\vec{B}_{\text{eff}}(\vec{R}_i)$, and \vec{B}_i a spatially varying magnetic field. At the end of the calculation \vec{B}_i is replaced by the true field acting on the sample, i.e., in the present case by a constant field in z direction. By differentiating Eq. (A4) one obtains

$$\frac{\partial \langle S_i^\alpha \rangle}{\partial B_j^\beta} = -S \frac{\partial B_S}{\partial x_i} \frac{\partial x_i}{\partial B_j^\beta} u_i^\alpha - SB_S \frac{\partial u_i^\alpha}{\partial B_j^\beta}. \quad (\text{A5})$$

For the sake of the simplicity we limit consideration here to the longitudinal fluctuations and neglect the last term which describes the transversal fluctuations. Thus

$$\begin{aligned} \frac{\partial \langle S_i^\alpha \rangle}{\partial B_j^\alpha} &= -S \frac{\partial B_S}{\partial x_i} \frac{\partial x_i}{\partial B_j^\alpha}, \\ \frac{\partial^2 \langle S_i^\alpha \rangle}{\partial B_m^\alpha \partial B_j^\alpha} &= -S \left(\frac{\partial^2 B_S}{\partial x_i^2} \frac{\partial x_i}{\partial B_m^\alpha} \frac{\partial x_i}{\partial B_j^\alpha} + \frac{\partial B_S}{\partial x_i} \frac{\partial^2 x_i}{\partial B_m^\alpha \partial B_j^\alpha} \right), \end{aligned} \quad (\text{A6})$$

etc. From Eq. (A4)

$$\frac{\partial x_i}{\partial B_j^\alpha} = \frac{g\mu_B S}{k_B T} \left(-\frac{2}{g\mu_B} \sum_m I(\vec{R}_i - \vec{R}_m) \frac{\partial \langle S_m^\alpha \rangle}{\partial B_j^\alpha} + \delta_{i,j} \right), \quad (\text{A7})$$

$$\frac{\partial^2 x_i}{\partial B_m^\alpha \partial B_j^\alpha} = \frac{g\mu_B S}{k_B T} \left(-\frac{2}{g\mu_B} \sum_n I(\vec{R}_i - \vec{R}_n) \frac{\partial^2 \langle S_n^\alpha \rangle}{\partial B_m^\alpha \partial B_j^\alpha} \right),$$

etc. Using the Fourier transforms

$$\begin{aligned} C^{(n)}(S^z(\vec{q}_1), \dots, S^z(\vec{q}_n)) \\ = \sum_{\vec{R}_1, \dots, \vec{R}_n} e^{i\vec{q}_1 \cdot \vec{R}_1} \times \dots \times e^{i\vec{q}_n \cdot \vec{R}_n} \\ \times C^{(n)}(S_1^z, \dots, S_n^z), \end{aligned} \quad (\text{A8})$$

one obtains from Eqs. (A6) and (A7)

$$\begin{aligned} C^{(2)}(S^z(\vec{q}_1), S^z(\vec{q}_2)) \\ = NS^2 \frac{\partial B_S}{\partial x} f(\vec{q}_1) \delta_{\vec{q}_1 + \vec{q}_2, 0} C^{(3)}(S^z(\vec{q}_1), S^z(\vec{q}_2), S^z(\vec{q}_3)) \\ = -NS^3 \frac{\partial^2 B_S}{\partial x^2} f(\vec{q}_1) f(\vec{q}_2) f(\vec{q}_3) \delta_{\vec{q}_1 + \vec{q}_2 + \vec{q}_3, 0}, \end{aligned} \quad (\text{A9})$$

where

$$f(\vec{q}) = 1 / \left(1 - \frac{2S^2}{k_B T} I(\vec{q}) \frac{\partial B_S}{\partial x} \right). \quad (\text{A10})$$

In higher orders the expressions for the C functions become more complicated. However, noticing that in the paramagnetic region, $\partial x_i / \partial B_i^\alpha \approx 1$ but $\partial^2 x_i / \partial B_m^\alpha \partial B_j^\alpha \approx T_C / T$, one can neglect terms of the type $(\partial x_i / \partial B_i^\alpha) (\partial^2 x_i / \partial B_m^\alpha \partial B_j^\alpha)$ at least far from T_C . Then one obtains generally

$$\begin{aligned} C^{(n)}(S^z(\vec{q}_1), \dots, S^z(\vec{q}_n)) \\ = N(-S)^n \frac{\partial^{n-1} B_S}{\partial x^{n-1}} f(\vec{q}_1) \times \dots \times f(\vec{q}_n) \\ \times \delta_{\vec{q}_1 + \dots + \vec{q}_n, 0}, \quad n > 2. \end{aligned} \quad (\text{A11})$$

This gives a simple structure for the correlation functions, useful in a perturbation expansion.

- ¹S. Methfessel and D. C. Mattis, in *Encyclopedia of Physics*, edited by S. Flügge (Springer, Berlin, 1968), Vol. XVIII/1, p. 389.
²C. Haas, *Crit. Rev. Solid State Sci.* **1**, 47 (1970).
³T. Kasuya, *Crit. Rev. Solid State Sci.* **3**, 131 (1972).
⁴P. Wachter, *Crit. Rev. Solid State Sci.* **3**, 189 (1972).
⁵E. L. Nagaev, *Phys. Status Solidi B* **65**, 11 (1974).
⁶C. Haas, *Phys. Rev.* **168**, 531 (1968).
⁷F. Rys, J. S. Helman, and W. Baltensperger, *Phys. Kondens. Mater.* **6**, 105 (1967).
⁸S. Alexander, J. S. Helman, and I. Balberg, *Phys. Rev. B* **13**, 304 (1976).
⁹J. Sinkkonen, *Phys. Rev. E* **19**, 6407 (1979).
¹⁰I. Balberg, *J. Phys. (Paris)* **41**, Suppl. 6, 75 (1980).
¹¹W. Nolting, *Phys. Status Solidi B* **79**, 573 (1977).
¹²W. Nolting, *J. Phys. C* **11**, 1427 (1978).
¹³W. Nolting, *Phys. Status Solidi B* **96**, 11 (1979).
¹⁴A. Rangette, A. Yanase, and J. Kübler, *Solid State Commun.* **12**, 171 (1973).
¹⁵A. Rangette, *Phys. Status Solidi B* **71**, 569 (1975).

- ¹⁶K. Kubo, *J. Phys. Soc. Jpn.* **36**, 32 (1974).
¹⁷P. Soven, *Phys. Rev.* **156**, 809 (1967).
¹⁸F. Yonezawa and K. Morigaki, *Suppl. Prog. Theor. Phys.*, No 53, 1 (1973).
¹⁹R. J. Elliot, J. A. Krumhansl, and P. L. Leath, *Rev. Mod. Phys.* **46**, 456 (1974).
²⁰H. Ehrenreich and L. M. Schwartz, in *Solid State Physics*, edited by H. Ehrenreich, F. Seitz, and D. Turnbull (Academic, New York, 1976), Vol. 31, p. 149.
²¹D. N. Zubarev, *Usp. Fiz. Nauk SSSR* **71**, 71 (1960) [*Sov. Phys. Usp.* **3**, 320, (1960)].
²²D. N. Zubarev, *Nonequilibrium Statistical Thermodynamics* (Consultants Bureau, New York, 1974).
²³L. Schwartz and E. Siggia, *Phys. Rev. B* **5**, 383 (1972).
²⁴P. G. de Gennes and J. Villain, *J. Phys. Chem. Solids* **13**, 10 (1960).
²⁵P. L. Leath, *Phys. Rev.* **171**, 725 (1968).
²⁶L. Schwartz and H. Ehrenreich, *Ann. Phys.* **64**, 100 (1971).

- ²⁷L. M. Roth, Phys. Rev. B 7, 4321 (1973).
- ²⁸M. Watabe and F. Yonezawa, Phys. Rev. B 11, 4753 (1974).
- ²⁹S. J. Cho, Phys. Rev. B 1, 4589 (1970).
- ³⁰K. Lendi, Phys. Condens. Matter 17, 189 (1974).
- ³¹G. Güntherodt, Phys. Condens. Matter 18, 37 (1974).
- ³²P. Wachter, in *Handbook on the Physics and Chemistry of Rare Earths*, edited by K. A. Gschneider, Jr. and L. Eyring (North-Holland, New York, 1979), Vol. 2, p. 507.
- ³³J. I. Pankove, *Optical Processes in Semiconductors* (Prentice-Hall, New Jersey, 1971), p. 63.